The International Journal of Advanced Manufacturing Technology (2019) 104:4421–4431
https://doi.org/10.1007/s00170-019-04228-6

ORIGINAL ARTICLE

Finite element analysis and simulation study of CFRP/Ti stacks using ultrasonic additive manufacturing

Sagil James [1] · Lenny De La Luz [1]

Received: 22 April 2019 / Accepted: 31 July 2019 / Published online: 22 August 2019

Abstract

The hybrid laminar composite stack of carbon fiber reinforced polymer (CFRP) and titanium (Ti) are widely used in several critical engineering applications, including aerospace and automobile sectors. The joining of CFRP and Ti through conventional methods has several limitations such as weight additional, material damage, and lower fatigue life. Ultrasonic additive manufacturing (UAM) is a solid-state manufacturing process capable of joining layers of dissimilar materials. Experimental studies have successfully demonstrated the welding of CFRP and Ti through UAM process. However, there is a lack of understanding of the exact bonding process and influence of process parameter on weld quality during UAM. The present study investigates the bonding process and the effects of critical parameters in the UAM process of CFRP and Ti layers using finite element analysis and simulation technique. The simulation study reveals that the CFRP/titanium stacks encounter interfacial cyclic shear stresses and shear strains. The study found that the vibrational amplitude and surface roughness of the substrates play a critical role in achieving a proper weld. The simulation results are validated using experimentation. The finding of this study can help advance the commercialization of UAM process for welding dissimilar materials and composites.

Keywords CFRP · Ultrasonic additive manufacturing · Titanium

1 Introduction

Carbon fiber is an advanced engineering material which is in high demand. It has several excellent material properties including high fatigue resistance, low thermal expansion coefficient, and superior strength [1]. Carbon fiber is often embedded in a matrix of polymer resin to form carbon fiber reinforced polymer (CFRP). While CFRP is an advanced composite, it has several limitations, including limited load-bearing capability and low wear resistance [1]. These problems are overcome by sandwiching CFRP with a thin layer of metal such as titanium (Ti) to form CFRP/Ti hybrid composite stack. It enhances its wear resistance, strength-to-weight ratio, and elastic modulus without much increase in weight [2]. CFRP/Ti hybrid stacks are an excellent choice for several engineering applications including aerospace, automotive, biomedical, electronics, and communications replacing traditional material such as steel and aluminum [3, 4].

CFRP and Ti layers are commonly joined together with adhesives. However, most adhesives are incapable of withstanding high temperatures and thereby limits the application of the hybrid composite stacks [5]. Another common practice is to join using rivets and bolts. The rivets might not handle the necessary load for high load-bearing components and also adds to the weight of the assembly [6]. Ultrasonic additive manufacturing (UAM) is a solid-state manufacturing welding process that has been developed recently [7]. UAM process is a derivative of the more popular ultrasonic welding technology [8]. However, unlike ultrasonic welding, UAM process can join multiple layers of materials, including dissimilar materials, to create three-dimensional (3D) structures [9–11]. UAM processes traditionally involve a sonotrode that vibrates with a frequency of 20 kHz or above [6]. UAM uses relatively low power and a minimal amount of heat compared with other joining process and, consequently, there is no change in the substrate's material properties or behavior [12]. These characteristics make UAM the preferred joining methods to create 3D composite structures of dissimilar materials.

✉ Sagil James
sagiljames@fullerton.edu

[1] Department of Mechanical Engineering, California State University Fullerton, Fullerton, CA 92831, USA

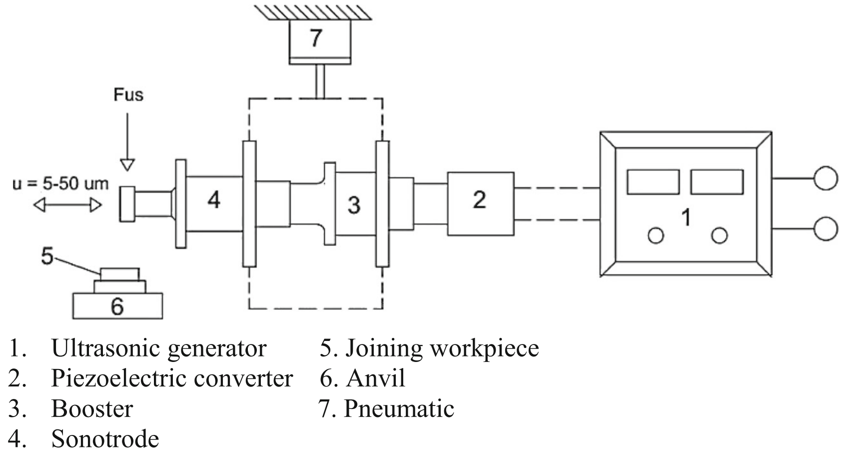

Fig. 1 Schematic of the ultrasonic additive manufacturing process

In the past, our research group has used the UAM process to weld CFRP/Ti stacks successfully [5]. While UAM is a beneficial process in joining dissimilar materials, its engineering applications are limited by a lack of clear understanding of the bonding mechanism involved [13, 14]. Previous studies have reported on the bonding mechanism of the ultrasonic welding process. One of the studies performed by Gao and Doumanidis [15] used finite element analysis (FEA) on the ultrasonic spot welding process. The study used frictional boundary conditions at the interface of weld layers and could explain the role of ultrasonic energy in obtaining proper weld. In another study, Zhang and Li [16] used a 3D FEA model for investigating the mechanical behavior of the substrate during the ultrasonic consolidation process. The study concluded that the cyclic vibrations cause dynamic stress at the interface. Abubaker et al. [17] performed a parametric study on the ultrasonic consolidation process with an aluminum workpiece and silicon carbide (SiC) fiber using FEA software ABAQUS. It is concluded that increasing high frequency and amplitude enhances the heat generation at the interface.

Our research group has studied the UAM process of CFRP/Ti stacks through experimentation [5]. The experimental study showed successful bonding of stacks of CFRP/Ti. The experimental study showed successful bonding of stacks of CFRP/Ti. However, experimental studies are not capable of explaining the complex and dynamic material deformation process happening between the substrate layers in real time. Researchers often resort to the use of simulation techniques to analyze such uncertain, non-linear, and dynamic systems [18, 19]. FEA studies have the capability of monitoring the microscopic material deformation mechanisms during the process. The FEA technique was used to conduct preliminary studies on the UAM process of welding a single stack of CFRP and Ti [5]. The study suggested that cyclic shear stresses caused plastic strains during the joining process. However, the preliminary study only considered a single process setting during the simulation. The effect of various process parameters was not considered in the preliminary study. The present study aims to extend the findings of the preliminary study and to investigate the underlying process mechanisms in UAM process along with understanding the effect of critical process parameters on the joining of CFRP/Ti stacks using UAM. The study

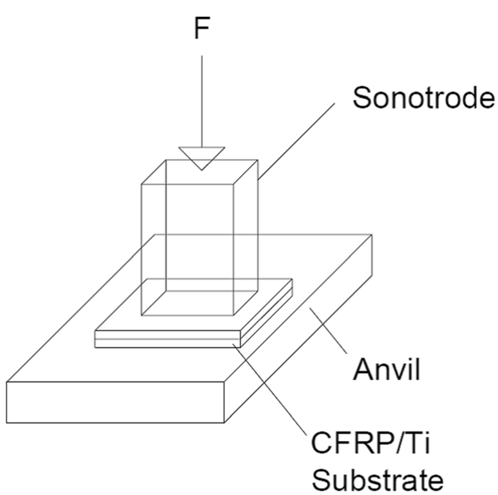

Fig. 2 Schematic of the UAM process on CFRP/Ti stacks

Fig. 3 In-house built experimental setup of UAM on CFRP/Ti stacks [14]

Table 1 Experiment parameters of UAM process

Parameters	Units	Values
CFRP thickness	μm	600
Ti thickness	μm	100
Frequency	kHz	20
Amplitude	μm	Variable
Surface roughness		Variable

considers the effect of vibrational amplitude and the frictional coefficient between the surfaces. A two-dimensional FEA model is developed using MSC Marc software and is used to analyze the bonding mechanism UAM process. The findings of the simulation study are then validated through experimentation.

2 Experimental study

Figure 1 shows the schematic of the UAM machining setup. The set up contains a sonotrode, transducer, and booster. Figure 2 shows the schematic of the UAM process of joining CFRP/Ti stacks. The experiments are performed using an in-house built UAM setup. A 1-kW Dukane system is used to power the system. The power is converted from low energy signals to a 20-kHz frequency. The frequency is transformed into a piezoelectric converter. The frequency transforms into high-frequency ultrasonic vibrations. A booster amplifies the mechanical vibrations from the converter. The ultrasonic vibrations are then transmitted to the tool and then to the substrates. The in-house fabricated experimental setup is shown in Figure 3.

The ultrasonic power supply can control the sonotrode amplitude by adjusting the voltage output. The CFRP and Ti substrates have thicknesses of 600 μm and 100 μm, respectively. Table 1 lists the material parameters for the experimental study.

The layers of CFRP/Ti substrates were welded successfully together. The welded CFRP/Ti stacks are shown in Fig. 4. After welding, it is observed that there were no signs of melting, thus suggesting solid-state welding. There were no signs of a reduction in material thickness in both the CFRP and titanium layers.

3 Finite element modeling and simulation

In this study, the FEA technique is utilized to investigate the process mechanism involved in UAM of the CFRP/Ti stacks. FEA is performed using MSC Marc Mentat software. A two-dimensional (2D) FEA is performed by simulating one anvil, Ti, CFRP, and sonotrode (tool). A two-dimensional (2D) simulation model is created, as shown in Fig. 5. The simulation consists of a sonotrode, CFRP layer, Ti layer, and an anvil. The sonotrode is made of Ti material. The anvil is made of cast iron and is used to provide support for the CFRP and Ti layers. The CFRP and Ti are rectangular having dimensions of 150 mm × 25 mm with a mesh of 10 × 3 triangular elements.

The CFRP is modeled as an orthotropic material as its material properties are different along the three mutually orthogonal directions. It is simulated as six layers with the following orientation, [0°, 90°, 0°, 90°, 0°, 90°]. The fiber orientations are chosen such a way that it matches the structure used in the experimental study described in the previous section. Figure 6 shows a snapshot of the CFRP model used for the FEA study. It should be noted that the multiple layers represent the individual orientations of the fibers which form one single stack as a woven fabric. The Ti is modeled as an isotropic material having its material properties identical in all directions. Gravity force of 9.8 m/s^2 is applied to the substrate in the negative Y direction. The sonotrode has a shape of 200 mm × 50 mm. It consists of a mesh of 10 × 10 elements. 4-node isoparametric, quadrilateral plane strain elements (element type 11) is used with geometric and material nonlinearity for the sonotrode, anvil, and Ti substrate. 4-node, plane strain, composite element (element type 151) is used for modeling the CFRP substrate. The automatic global remeshing feature in MSC Marc is used to increase the accuracy of the simulation and reduce computational time. The sonotrode is considered as a rigid body in the simulation. Three different coefficients of friction (0.4, 0.5, and 0.6) are considered at the interface between the CFRP and Ti substrate

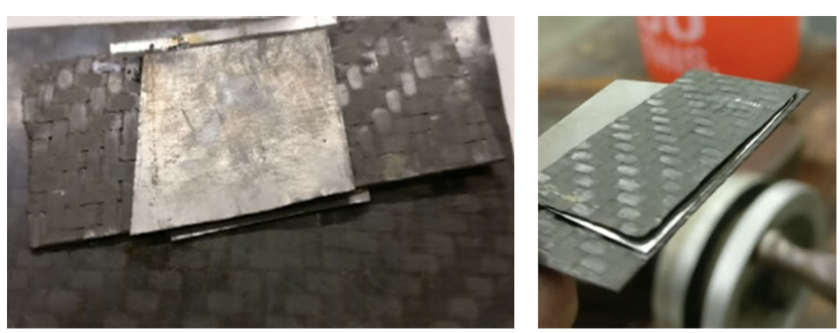

Fig. 4 CFRP/Ti stacks welding using UAM process

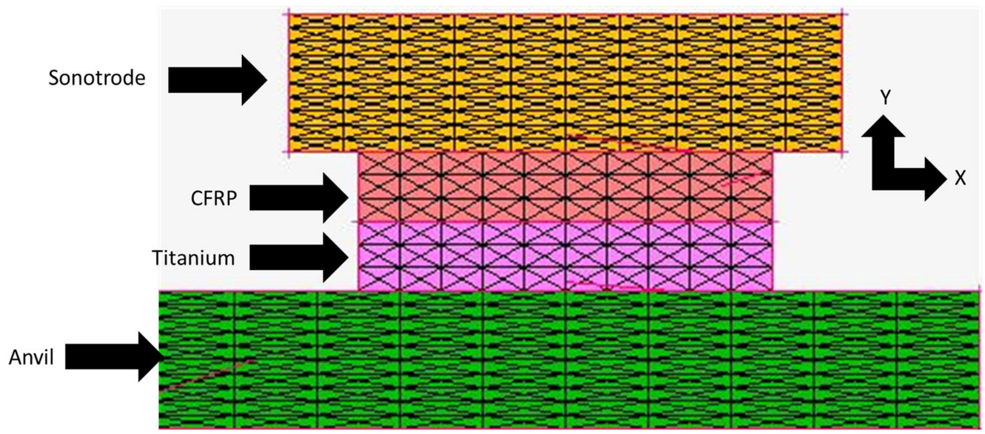

Fig. 5 Finite element model in MSC Marc

layers. Also, three vibrational amplitudes (10, 30, and 50 μm) are considered for the tool. The anvil is fixed in both X and Y directions. A static load of 150 N is continuously applied using the sonotrode normal to the substrate layers. The sonotrode vibrates parallel to the workpieces in both positive and negative X direction. The sonotrode vibrates as a sine wave function with the displacement $X(t)$ expressed as:

$$X(t) = \text{Amplitude} \times \text{Sin}(2 \times \pi \times \text{Frequency} \times t) \qquad (1)$$

where t is the time. The FEA model is simulated for a duration of 4 ms. The model is then subject to a shear test for a duration of 1 ms. Table 2 shows the parameters used for the current simulation study.

4 Results and discussions

Figure 7 shows the snapshot of the FEA simulation results for UAM of CFRP/Ti stacks using an amplitude of 30 μm and a coefficient of friction of 0.5 after 4 ms. The figure suggests that both CFRP and Ti undergo deformation during the UAM

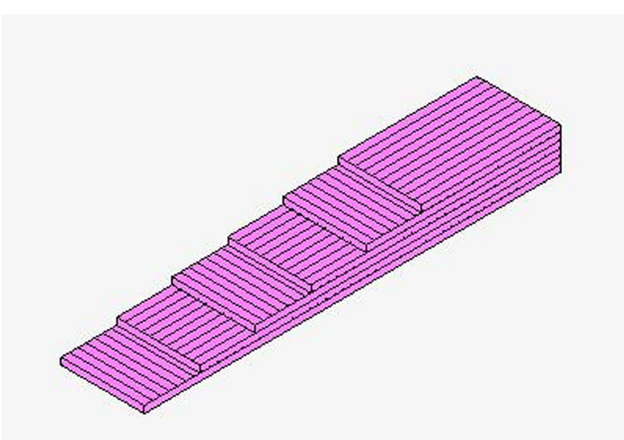

Fig. 6 Finite element model of CFRP

process. As the simulation progress, a global adaptive remeshing is performed at critical regions of the substrate undergoing large strains. Further, the shear stress and shear strain distributions in the CFRP and Ti substrates are analyzed. A performance comparison between the relative strengths of the UAM process and the conventional techniques (including riveting, bolting, gluing) is beyond the scope of the current study.

4.1 Variation in shear stress

Figure 8 shows the variations of interfacial shear stresses with respect to time during the UAM process. Three different amplitudes of 10, 30, and 50 μm are used which are considered as low, medium, and high respectively. The coefficient of frictional value used here is 0.5. The interfacial shear stresses are caused by the relative cyclic motion of the tool on the substrate layers along with the applied static load. The figure suggests that the interfacial shear stress values undergo repeated fluctuations as the simulation progresses. It is also seen that the magnitude of the interfacial shear stress increases with an increase in amplitude. Figure 9 shows the distribution of shear stress on the CFRP and Ti substrates. Peak values of shear stresses are seen at the interface between the two layers. High shear stress values are also observed in the sonotrode/

Table 2 Parameters for finite element analysis simulation of UAM process

Parameters	
Workpiece	CFRP (150 mm × 25 mm) Ti (150 mm × 525 mm)
Temperature	298 K
Ultrasonic frequency	20 KHz
Amplitude	10, 30, 50 μm
Coefficient of friction	0.4, 0.5, 0.6
Static load	150

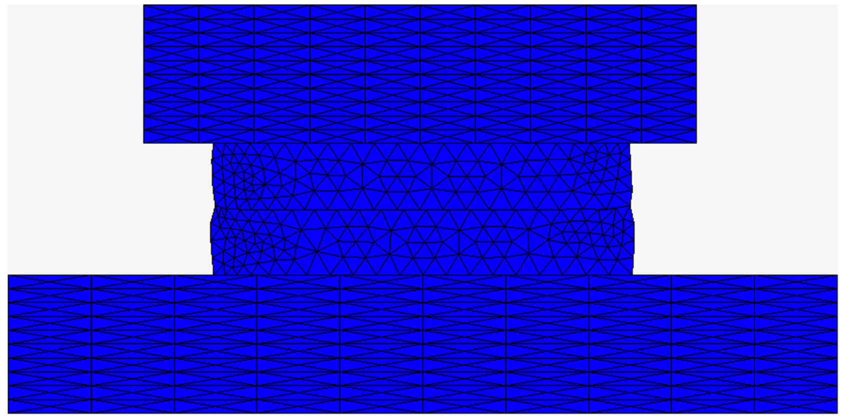

Fig. 7 CFRP/Ti substrates after UAM process

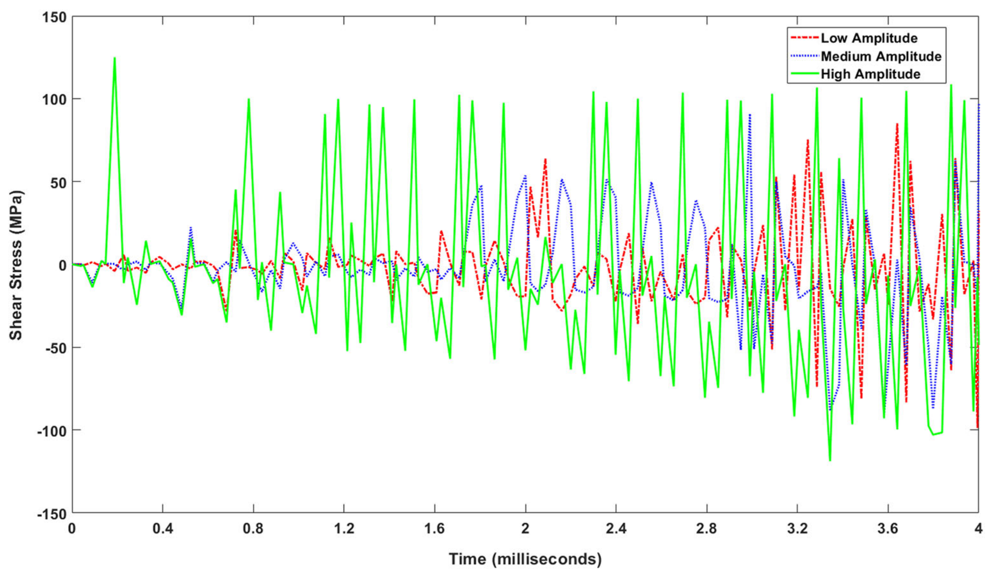

Fig. 8 Variation in interfacial shear stress with time

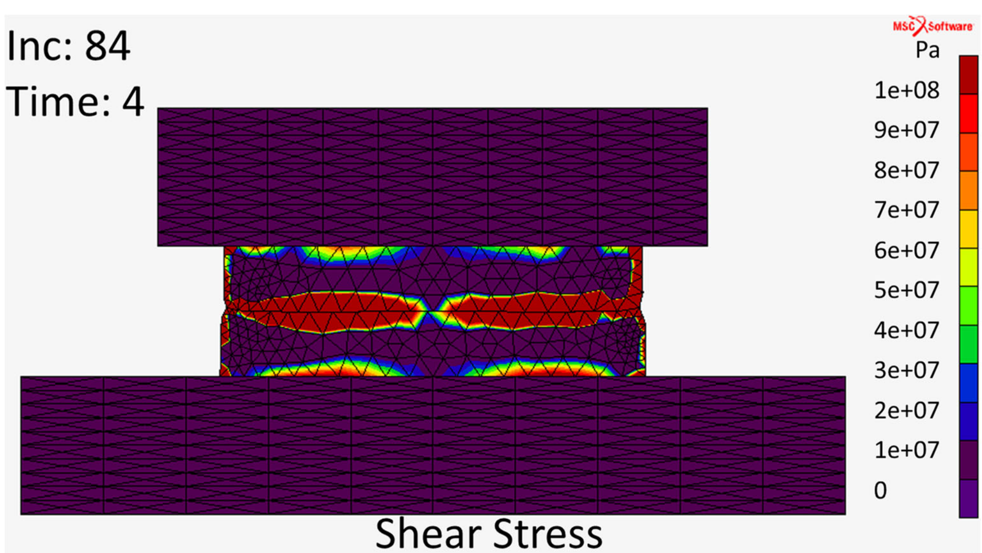

Fig. 9 Distribution of shear stress during UAM process

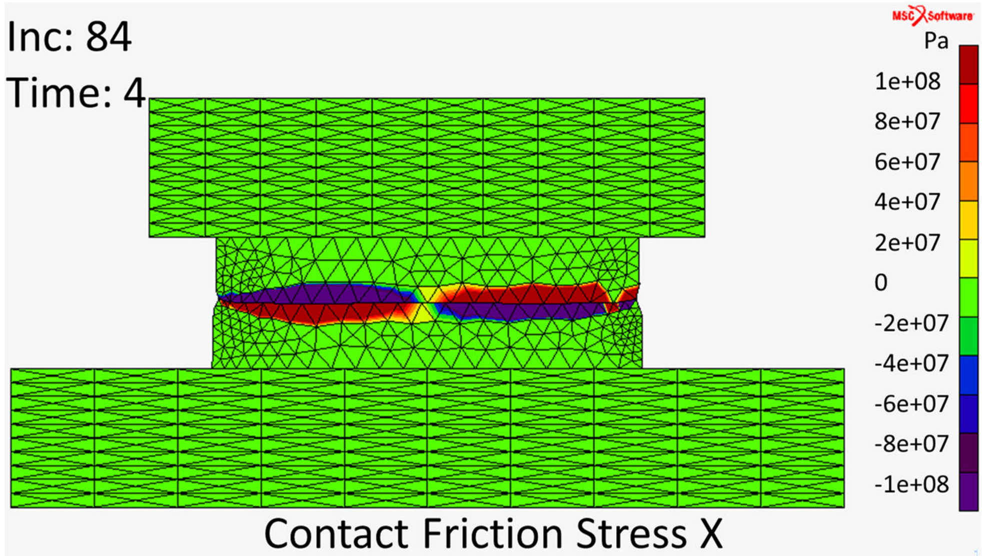

Fig. 10 Distribution of contact frictional stress during UAM process

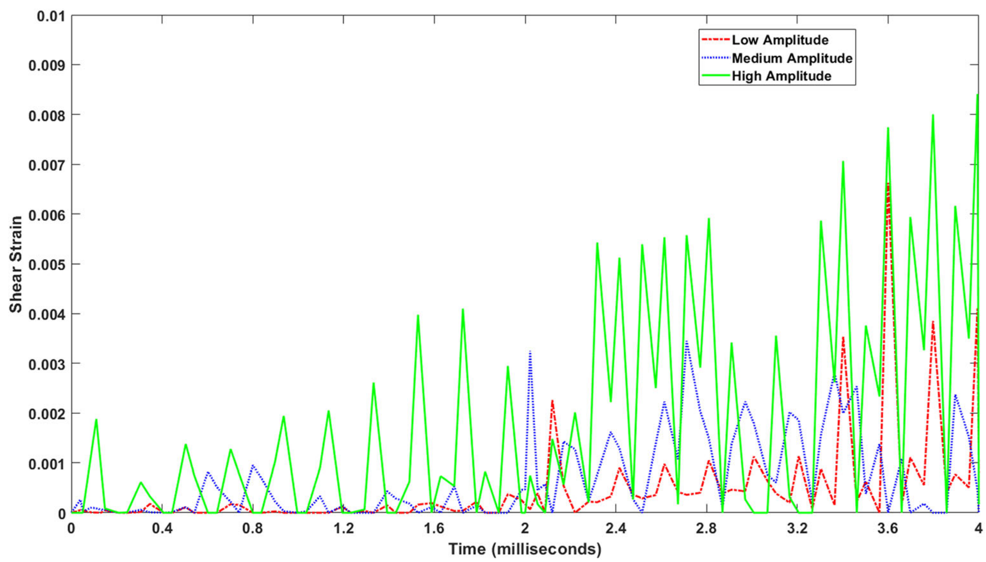

Fig. 11 Variation in interfacial shear strain with time

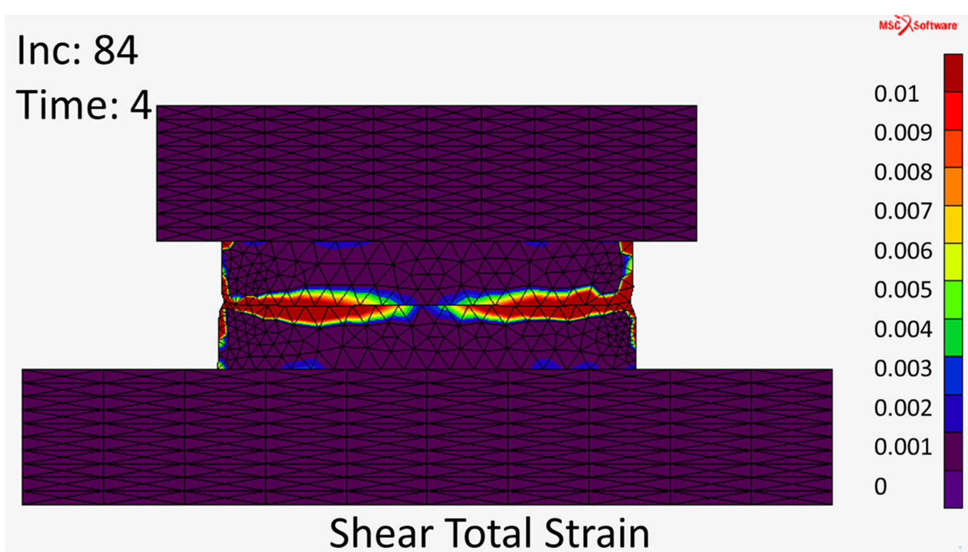

Fig. 12 Distribution of shear strain during UAM process

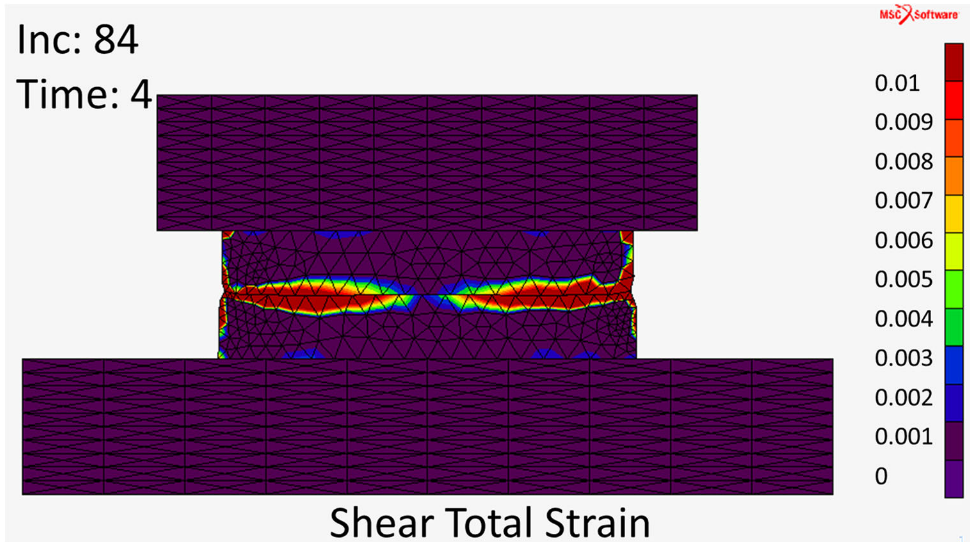

Fig. 13 Distribution of plastic shear strain during UAM process

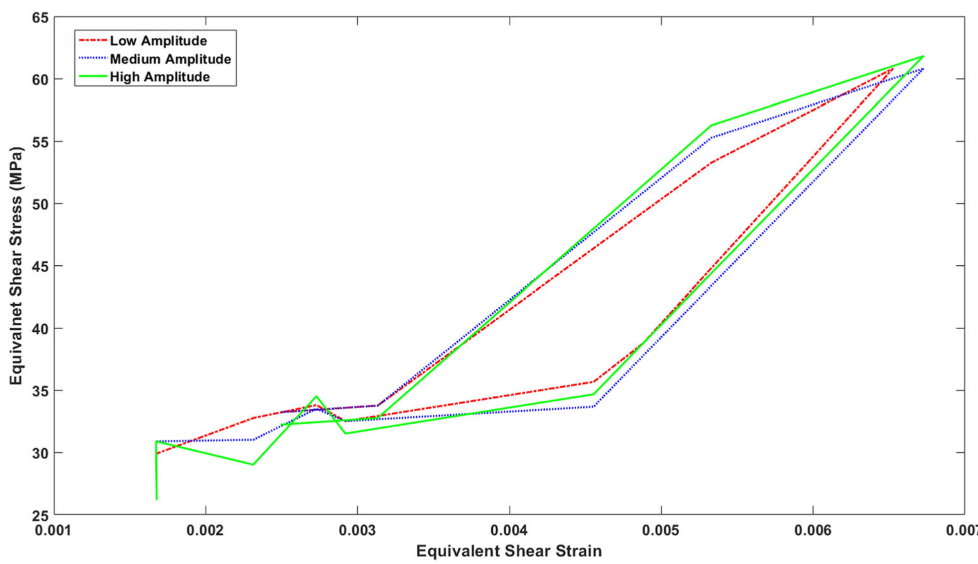

Fig. 14 Shear stress-shear strain curve

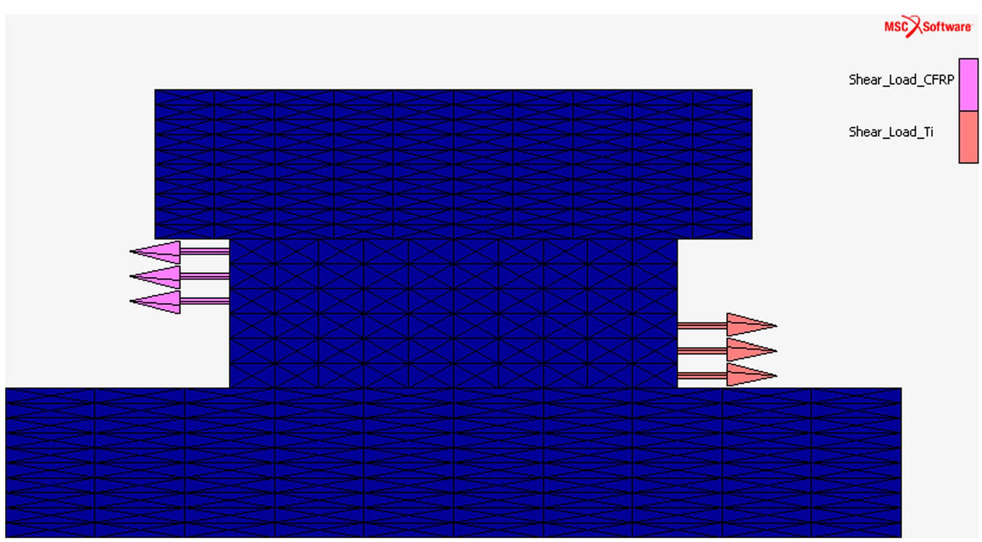

Fig. 15 Shear testing of the welded CFRP/Ti substrates

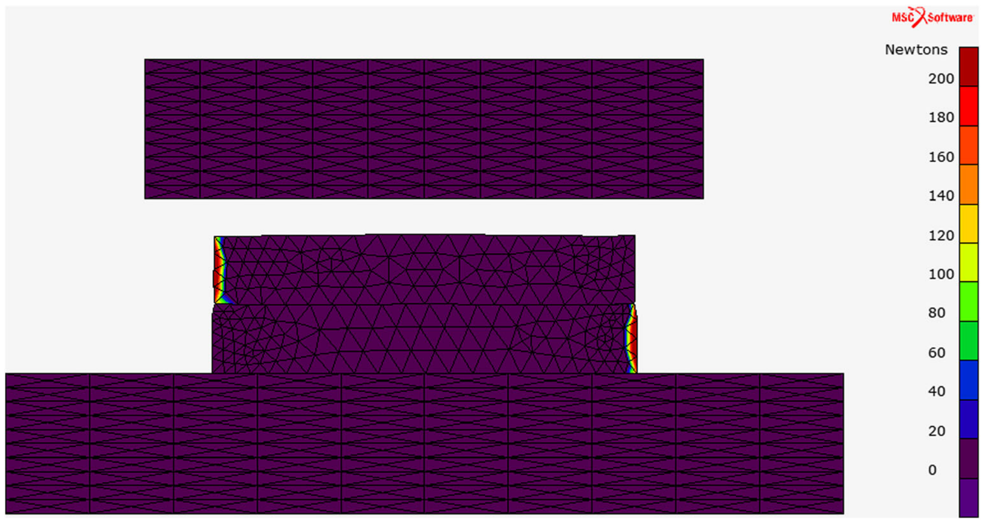

Fig. 16 Distribution of external forces during shear testing

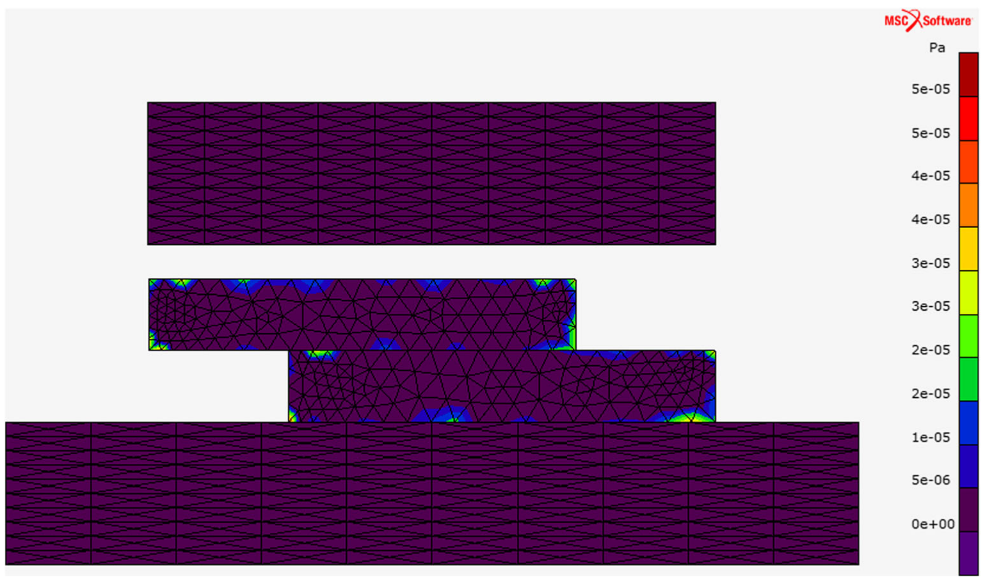

Fig. 17 Distribution of shear stress on the substrates at the end of testing

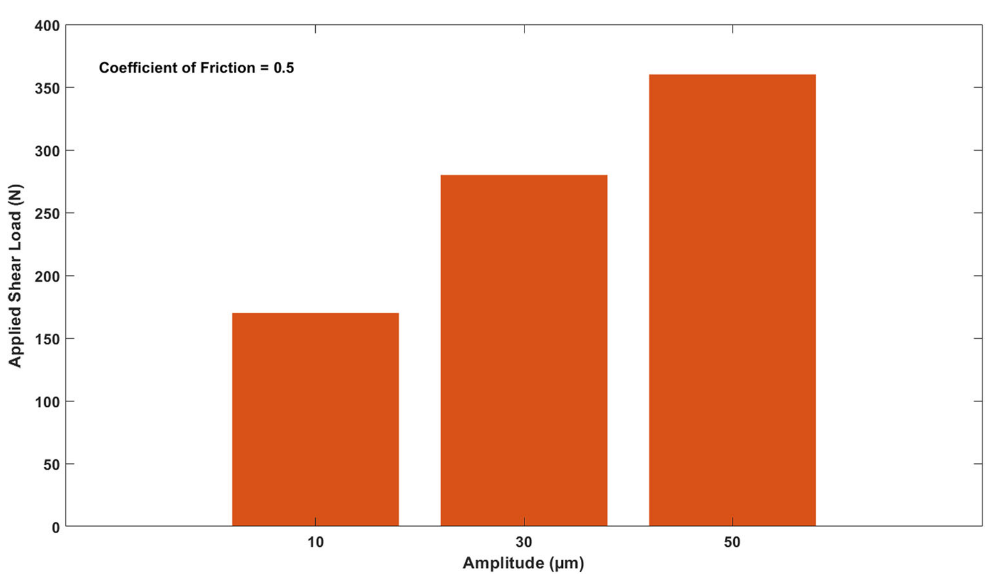

Fig. 18 Variation in critical shear load with respect to the amplitude

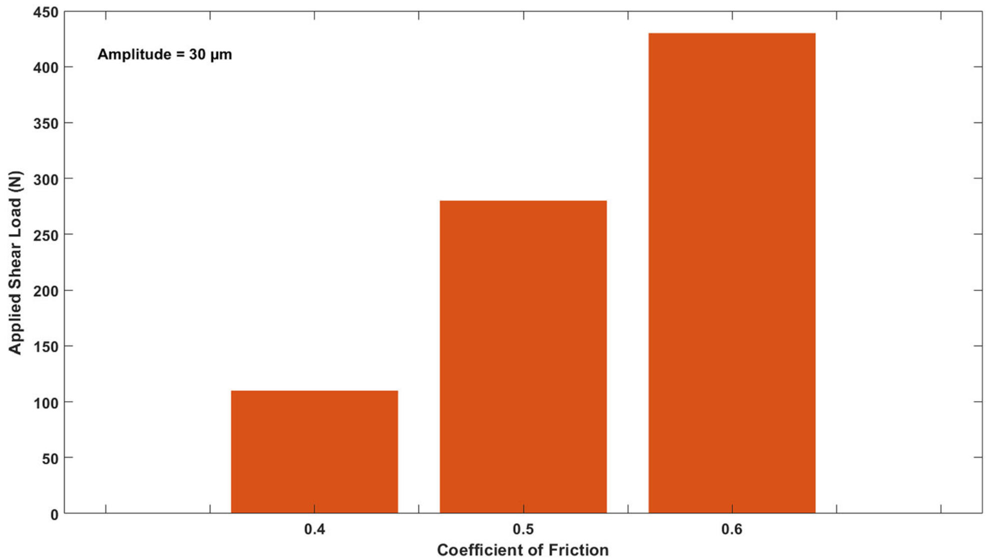

Fig. 19 Variation in critical shear load with respect to the friction

CFRP and anvil/Ti interfaces. Figure 10 shows the distribution of the contact frictional stresses during the UAM process. It is observed that the frictional stress is concentrated between the CFRP/Ti interface. It suggests that friction plays a critical role in joining of the substrates during the UAM process.

4.2 Variation in shear strain

The repeated variations in interfacial shear stress result in significant deformation at the interface between the CFRP and Ti substrates. The variation in interfacial shear strain with respect to time is shown in Fig. 11. The coefficient of friction sued in this case is 0.5. From the figure, it is seen that the magnitude of the interfacial shear strain increases as the simulation progresses. Moreover, the shear strain values increase with an increase in amplitude. Figure 12 shows the distribution of shear strain on the CFRP and Ti substrates during the UAM process. The figure suggests that the interfacial element undergoes significant deformation during the UAM process. The large deformation of the interfacial element is critical in achieving proper welding of the substrate layers. Figure 13 shows the distribution of the plastic strain during the UAM process. The figure suggests that only Ti substrate undergoes plastic deformation during the joining process. The plastic deformation is found higher in the center of the Ti substrate and lesser towards the edges.

Fig. 20 Lap shear testing of CFRP/Ti substrates

4.3 Shear stress-shear strain curve

Figure 14 shows the shear stress-shear strain curve during the UAM process of the CFRP/Ti substrates. A coefficient of friction value of 0.5 is used for this study. It can be seen that the equivalent shear stress increases gradually, and then it decreases considerably with equivalent strain. The figure resembles the Bauschinger effect in which the strength of the substrate decreases due to the cyclic reversal of the shear strains. The stress-strain response follows the direction in which the sonotrode applies shear stress on the substrates. It suggests that the dynamic stress distribution within the substrate causes plastic instability, which helps in joining the substrate layers.

4.4 Shear testing of simulation model

The shear testing of the CFRP/Ti model is conducted by subjecting it to varying shear loading for a duration of 1 ms, as shown in Fig. 15. The shear test is performed after the completion of the UAM process (4 ms). At the start of the shear testing, the static load is withdrawn, and the sonotrode is lifted vertically upwards, as shown in Fig. 16. The CFRP layer is pulled to the left while the Ti layer is pulled to the right causing a resulting interfacial shearing of the substrates. The

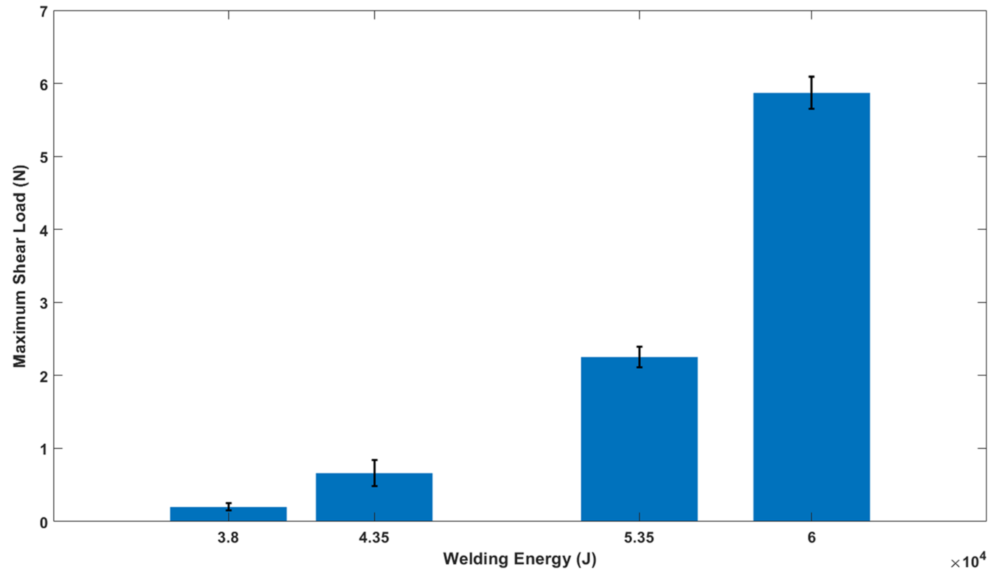

Fig. 21 Experimental results for maximum shear load vs. welding energy

applied shear load is gradually increased until the substrates separate and slip against each other, as shown in Fig. 17.

The variation in critical shear load with respect to different vibrational amplitudes is shown in Fig. 18. The coefficient of friction is maintained at 0.5. It is seen that the higher amplitudes cause stronger welding between the substrate layers. It is because the increasing amplitude increases the energy generated at the interface aiding stronger welding. Figure 19 shows the variation in critical shear load for varying coefficient of friction values and vibration amplitude of 30 μm. It is evident that the frictional coefficient has a positive impact on the welding process during the UAM process. It suggests that the surface roughness of the substrate layers is critical in for achieving strong welds during the UAM process.

5 Validation of simulation results with experimentation

The results of the FEA simulation study are validated through experimentation. During the experiments, the ultrasonic energy and the surface roughness of the substrate are varied. The ultrasonic energy represents the amplitude of vibration of the sonotrode. The maximum shear load is determined using a lap shear test performed on a digital force gauge (Make: Mark-10), as shown in Fig. 20. The variation in maximum shear load with respect to different welding energies is shown in Fig. 21. The experimental results suggest the welding energy or the vibrational amplitude has a positive influence on the weld strength. The result is consistent with the observations in the simulation. Figure 22 shows the variation in maximum shear

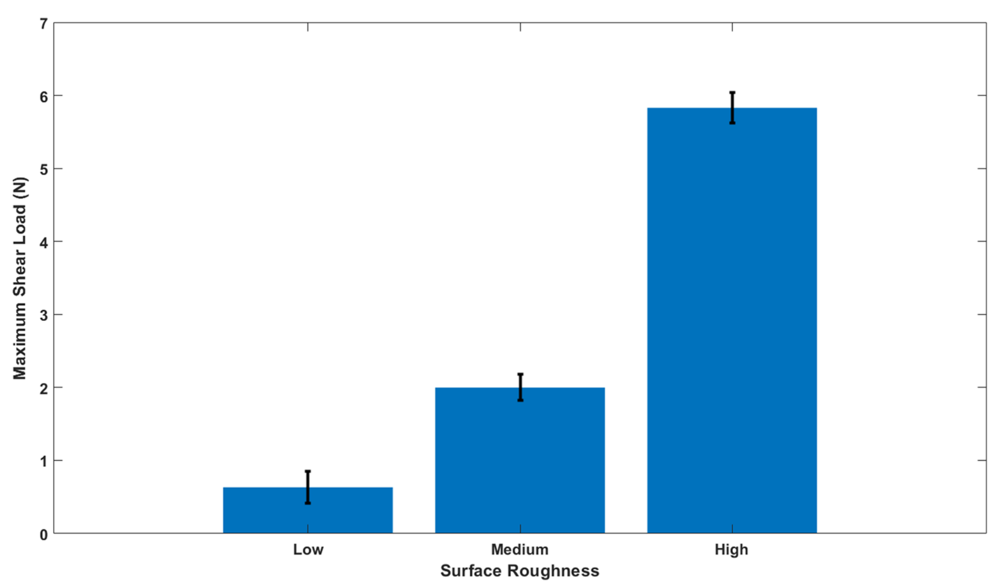

Fig. 22 Experimental results—maximum shear load vs. surface roughness

load with respect to varying surface roughness. The surface roughness is imparted on the Ti surface. The study considers three-surface roughness for the experiments, including low (smooth), medium (mild roughness), and high (very rough). The figure suggests that the critical shear load increases with an increase in surface roughness. Again, the results agree with the finding of the simulation.

6 Conclusion

In this study, ultrasonic additive manufacturing (UAM) of CFRP and Ti is investigated through finite element analysis (FEA) technique. The study investigates the effect of vibrational amplitude and surface roughness on the welding process. The conclusion drawn from the study are as follows:

a. The stress analysis showed the presence of interfacial shear stresses between the CFRP and Ti. The shear stress values undergo cyclic variations during the UAM process. The stress values increase with an increase in amplitude high contact frictional stresses are found on the interfacial elements.
b. Strain analysis showed that the interfacial elements undergo large deformations. The plastic strain is found only on the Ti substrate. The shear strain values increase with an increase in vibrational amplitude.
c. The shear stress-shear strain curve showed the presence of the Bauschinger effect, suggesting strength degradation as the UAM process continues.
d. The model is subject to shear test, and the critical shear load is measured. Both vibrational amplitude and coefficient of friction positively influence the weld strength.
e. The simulation results are validated through experimentation, and the experimental results are consistent with the finding of the simulation.

The results of this study would help advance the critical engineering applications of CFRP/Ti stacks in industries such as aerospace and defense. Further directions of this study would be to analyze multiple layers of CFRP/Ti materials and then integrating the results into the actual manufacturing process in real-time.

Funding information The authors received financial support from the College of Engineering and Computer Science at the California State University Fullerton.

References

1. Zhang L, Liu Z, Tian W, Liao W (2015) Experimental studies on the performance of different structure tools in drilling CFRP/Al alloy stacks. Int J Adv Manuf Technol 81(1-4):241–251
2. Lv J et al (2016) Study on process and mechanism of laser drilling in water and air. Int J Adv Manuf Technol:1–9
3. Sonate A, Vepuri D, James S (2017) Study of micro ultrasonic machining of CFRP/Ti stacks. in ASME 2017 International Mechanical Engineering Congress and Exposition. American Society of Mechanical Engineers
4. Tsao C (2008) Thrust force and delamination of core-saw drill during drilling of carbon fiber reinforced plastics (CFRP). Int J Adv Manuf Technol 37(1):23–28
5. James S et al (2018) Experimental and simulation study of ultrasonic additive manufacturing of CFRP/Ti Stacks. in ASME 2018 13th International Manufacturing Science and Engineering Conference. American Society of Mechanical Engineers
6. James S, Sonate A (2017) Experimental study on micromachining of CFRP/Ti stacks using micro ultrasonic machining process. Int J Adv Manuf Technol:1–9
7. Wolcott PJ, Dapino MJ (2017) Ultrasonic additive manufacturing. In: Additive Manufacturing Handbook: Product Development for the Defense Industry. CRC Press/Taylor and Francis Boca Raton, Florida
8. James S, Rajanna P (2018) Molecular dynamics simulation study of ultrasonic powder consolidation process. in ASME 2018 13th International Manufacturing Science and Engineering Conference. American Society of Mechanical Engineers
9. Dehoff R, Babu S (2010) Characterization of interfacial microstructures in 3003 aluminum alloy blocks fabricated by ultrasonic additive manufacturing. Acta Mater 58(13):4305–4315
10. Schick D et al (2010) Microstructural characterization of bonding interfaces in aluminum 3003 blocks fabricated by ultrasonic additive manufacturing-methods were examined to link microstructure and linear weld density to the mechanical properties of ultrasonic additive manufacturing. Weld J 89(5):105S
11. Friel RJ, Harris RA (2013) Ultrasonic additive manufacturing–a hybrid production process for novel functional products. Procedia CIRP 6:35–40
12. Sridharan N, Norfolk M, Babu SS (2016) Characterization of steel-Ta dissimilar metal builds made using very high power ultrasonic additive manufacturing (VHP-UAM). Metall Mater Trans A 47(5): 2517–2528
13. Fujii HT, Sriraman M, Babu S (2011) Quantitative evaluation of bulk and interface microstructures in Al-3003 alloy builds made by very high power ultrasonic additive manufacturing. Metall Mater Trans A 42(13):4045–4055
14. Parmar M, James S (2018) Experimental and Modeling study of liquid-assisted—laser beam micromachining of smart ceramic materials. J Manuf Mater Process 2(2):28
15. Doumanidis C, Gao Y (2004) Mechanical modeling of ultrasonic welding. Weld J-N Y 83(4):140-S
16. Zhang CS, Li L (2010) Effect of substrate dimensions on dynamics of ultrasonic consolidation. Ultrasonics 50(8):811–823
17. Abubakar AA, Khan SM, Mekid S (2017) On the modeling of fibers embedding in aluminum using ultrasonic consolidation. J Eng Mater Technol 139(3):031003
18. Sun K et al (2018) Adaptive fuzzy control for non-triangular structural stochastic switched nonlinear systems with full state constraints. IEEE Trans Fuzzy Syst
19. Qiu J, Sun K, Wang T, Gao H (2019) Observer-based fuzzy adaptive event-triggered control for pure-feedback nonlinear systems with prescribed performance. IEEE Trans Fuzzy Syst:1